

## SPECTRAL DIVERSITY OF TYPE IA SUPERNOVAE

J. BERIAN JAMES<sup>1,2</sup>, TAMARA M. DAVIS<sup>1</sup>, BRIAN P. SCHMIDT<sup>1</sup> AND ALEX G. KIM<sup>3</sup>

*Draft version February 19, 2006*

### ABSTRACT

We use published spectroscopic and photometric data for 8 Type Ia supernovae to construct a dispersion spectrum for this class of object, showing their diversity over the wavelength range 3700 Å to 7100 Å. We find that the B and V bands are the spectral regions with the least dispersion, while the U band below 4100 Å is more diverse. Some spectral features such as the Si line at 6150 Å are also highly diverse. We then construct two objective measures of ‘peculiarity’ by (i) using the deviation of individual objects from the average SN Ia spectrum compared to the typical dispersion and (ii) applying principle component analysis. We demonstrate these methods on several SNe Ia that have previously been classified as peculiar.

*Subject headings:* supernovae : general

### 1. INTRODUCTION

Type Ia supernovae (SNe Ia) are observed to display remarkably homogeneous light curves in broadband photometry. They are currently classified according to a single-parameter family of peak luminosity as a function of light curve shape (Phillips 1993), which allows them to be used as accurate cosmological distance indicators.

However, we know that this one-parameter family does not completely encompass the variety of SNe Ia observed. Once we have reduced any contribution from measurement error to the point where its effects are negligible the intrinsic diversity of SNe Ia themselves represent the limiting accuracy to which a one-parameter family can aspire.

This diversity manifests itself as differences in the SN Ia spectra. It is important to assess the diversity in particular features of SN Ia spectra and find those hot spots that have the most significant effect on the broadband photometry used for cosmology. Identifying these points of variability in SN Ia spectra has a multi-fold benefit. (1) It allows us to identify which spectral regions are the most stable for photometry and thus design future dedicated SN cosmology probes to utilise these stable wavelength regions. (2) It allows us to classify SN Ia based on certain spectral features into sub-types that have a tighter magnitude-redshift relation than the entire SN Ia population. (3) It allows us to put weighted error bars on the points in the magnitude-redshift relation depending on which part of a redshifted SN Ia spectrum was sampled by the filter set in use.

Recent work in this area includes Benetti et al. (2005), who investigate the diversity of SNe Ia and identify three possible sub-classes based on the evolution of their photospheric velocity, the temporal evolution of the Si II feature before maximum, and the decline rate parameter  $\Delta m_{15}(B)$ . Vaughan et al. (1995) made an early attempt to define a subset of SN Ia with very similar properties by providing a cut-off on the  $B-V$  colour at maximum that selected a subset with an observed dispersion of less than 0.25 mag. These were later called the ‘Branch Normal’ SNe Ia. Previous SN Ia spectral investigations include Nugent et al. (1995) who found that the ratio,

$\mathcal{R}(\text{Si II})$ , of two optical Si II features is related to the decline parameter  $\Delta m_{15}(B)$  and thus to the luminosity of the supernova. Benetti et al. (2004) found that while this relation holds for supernovae with  $\Delta m_{15}(B) > 1.2$  it may break down for supernovae with  $\Delta m_{15}(B)$  values smaller than this.

In this paper we assess the diversity in SN Ia spectral features near maximum light. In Section 2 we describe the data set and our analysis technique. In Section 3 we provide plots of the spectral variability of SNe Ia as a function of wavelength and discuss the features. In Section 4 we provide a prescription for determining the degree of ‘peculiarly’ of a supernova based on its spectrum near maximum light.

### 2. DATA PREPARATION

The sample consists of 18 previously published spectra taken for 8 low redshift type Ia SNe. Table 1 lists the spectra and the source catalogues. These represent the subset of published objects that are confirmed to be normal SNe Ia and have good quality spectra within two days of maximum light as well as established  $\Delta m_{15}$  values, B magnitudes at maximum light ( $M_B$ ), extinction values ( $E(B-V)$ ) and distance moduli ( $\mu_0$ ). Table 2 lists the photometric properties of the source objects.

Correction for dust extinction is made according to the standard extinction law of Savage & Mathis (1979), using colour excess values  $E(B-V)$  from Phillips et al. (1999) where available.

It is a familiar task to convert apparent magnitudes to absolute magnitudes in order to compare the brightness of objects at different distances. In order to compare the 18 spectra in our sample we have to perform the spectral equivalent of converting from apparent to absolute magnitude. We do this by multiplicatively scaling the spectra so they give the correct absolute magnitude in the B or V band after synthetic photometry.

There is more than one way to determine the ‘correct’ absolute magnitude. We could choose to scale each spectrum to the broadband magnitude of its source supernova, once corrected for extinction, distance modulus and  $\Delta m_{15}(B)$ . However the observational uncertainty on nearby SN Ia magnitudes is typically about 0.2 magnitudes, while the standard deviation in magnitude values is typically about 0.4 and 0.2 magnitudes in B and V respectively (Hamuy et al. 1996). This makes it difficult with the current data to distinguish broadband magnitude variations due to intrinsic spectral variability

<sup>1</sup> Research School of Astronomy and Astrophysics, Australian National University; tamarad,brian@mso.anu.edu.au

<sup>2</sup> School of Physics, University of Sydney; jbjames@physics.usyd.edu.au

<sup>3</sup> Lawrence Berkeley National Laboratory, Physics Division; AGKim@lbl.gov

TABLE 1  
CATALOGUE OF SNE IA SPECTRA USED IN THIS STUDY.

SN	epoch (days)	$\lambda_{\min}$ (Å)	$\lambda_{\max}$ (Å)	Reference <sup>a</sup>
1981B	0	1272	8392	Br83
1989B	-1	3001	11167	We94
1992A	-1	3564	7100	Ki93
1994D	-2	3402	9132	Pa96
	0	3069	10130	Br
	2	3466	9204	Pa96
	2	4439	7013	Pa96
1994S	0	3120	11300	Br
1996X	-2	3748	9917	Sal01
	0	3079	10670	Sal01
	1	3078	10669	Sal01
1998aq	0	3720	7500	Br03
	1	3720	7511	Br03
	2	3720	7521	Br03
1999ee	-2	3262	9983	Ha02
	-1	3559	9134	Ho
	0	3262	9687	Ha02

<sup>a</sup>REFERENCES.—Br83: Branch et al. 1983; Br03: Branch et al. 2003; Ha02: Hamuy et al. 2002; Ki93: Kirshner et al. 1993; Pa96: Patat et al. 1996; Sal01: Salvo

TABLE 2  
CATALOGUE OF PHOTOMETRIC PARAMETERS FOR SNE IA.

SN	$\Delta m_{15}(B)$	$B_{\max}$	$V_{\max}$	$E(B-V)$	$\mu_0$	References <sup>b</sup>
1981B	1.10(07)	12.00(02)	—	0.11(03)	30.10(30)	Br83
1989B	1.31(07)	12.34(05)	12.02(05)	0.34(04)	29.73(04)	We94
1992A	1.47(05)	12.60(20)	12.61(05)	0.00(02)	31.59(05)	Ph99; Le93
1994D	1.32(05)	11.84(05)	11.92(05)	0.00(02)	31.10(07)	Pa96; Ph99
1994S	1.10(10)	14.85(04)	14.84(06)	0.00(03)	34.36(03)	Kn03; Ph99
1996X	1.31(08)	13.24(02)	13.21(01)	0.01(02)	32.19(07)	Ph99; Sal01
1998aq	1.14(10)	12.39(05)	12.57(05)	0.014(05)	31.72(14)	Sah01; Br03
1999ee	0.94(06)	14.93(02)	14.68(15)	0.30(04)	33.55(23)	Ha02; St02

<sup>b</sup>REFERENCES.—Br83: Branch et al. 1983; Br03: Branch et al. 2003; Ha02: Hamuy et al. 2002; Kn03: Knop et al. 2003; Le93: Leibundgut et al. 1993; Pa96: Patat et al. 1996; Ph99: Phillips et al. 1999; Sah01: Saha et al. 2001; Sal01: Salvo et al. 2001; St02: Stritzinger et al. 2002; We94: Wells et al. 1994

from variations due to observational error.

Instead we choose to scale each spectrum to a fixed broad-band magnitude. This allows us to probe the spectral diversity without contamination from observational magnitude uncertainties. When we scale to a fixed magnitude we artificially minimise the diversity in that region. To examine the magnitude of this effect, we scale the spectra to fixed  $M_B$  in the first instance and to fixed  $M_V$  in the second. The choice of scaling has a small effect compared to the size of the spectral variations. The mean values of the B and V absolute magnitudes are  $M_B = -19.16 \pm 0.05$  and  $M_V = -19.11 \pm 0.02$  ( $1\sigma$ ), agreeing with the better performance of the Hamuy et al. (1996) relation in the V band.

Scaling in a single band is achieved by allowing for a linear relationship between the synthetic photometric magnitude and the logarithm of the scaling factor (luminosity)<sup>4</sup>,

$$M = a \log k + b, \quad (4)$$

The value of the slope constant  $a$  is constant for all objects

<sup>4</sup> A refinement of this technique is to fit to both  $M_B$  and  $M_V$  simultaneously, which creates a wider, more shallow dependence of variability on wavelength band, further reducing the intensity relative to the spectral variations. This is

within a particular band. The offset  $b$  varies depending on the units of the spectrum, and is determined for each object separately by computing the relation 4 for a range of scaling factors  $k$ . From this follows the relationship for  $k$  in terms of a fixed desired magnitude  $M$ .

With this process complete we have extinction-corrected SN Ia spectra that represents the most homogeneous spectral set we are able to generate. We now test these spectra for diversity in the sample.

### 3. MEASURING SN IA DIVERSITY

For each object we compile a single spectrum based on the average of all available spectra for that object between  $-2$  and  $2$  days from maximum. We use logarithmic bin spacing to offset the Doppler broadening of linewidths at higher wavelengths. The eight average spectra are binned to constant resolution,  $R = \lambda/\Delta\lambda$ , with bin size proportional to the bin centre,

$$\frac{\Delta\lambda}{\lambda} \approx \frac{v}{c} = \beta. \quad (5)$$

Our choice of  $\beta = 0.005$  corresponds to approximately  $20\text{Å}$  bins near  $4000\text{Å}$  and  $35\text{Å}$  bins near  $7000\text{Å}$ . This choice of binning parameter is narrow enough to appropriately sample all prominent spectral features, but wide enough to be insensitive to noise, allowing for effective synthesis of the spectra. We tested a variety of bin widths from  $\beta = 0.001$  to  $\beta = 0.02$  and the results are not sensitive to the width chosen.

Using the averaged spectra from the eight supernovae in our sample we calculate the overall mean spectrum and determine the root-mean-square (RMS) deviation from the mean in each bin to quantify the diversity in that region. The result is plotted in Figures 1 and 2, where the lower panel shows the overall average spectrum and the solid line in the middle panel shows the RMS dispersion about the mean. The shaded regions in this figure represent the uncertainty in the RMS dispersion, which is estimated by bootstrap resampling (Efron 1982).

We wish to isolate the intrinsic diversity of SNe Ia from observational scatter. As the spectra used in the sample range from epoch  $-2$  to  $2$  days we expect some diversity within the spectra for a single object. The observations themselves are also subject to observational scatter not ascribable to intrinsic diversity in the SN Ia population. We seek to quantify this variance and subtract it from the overall quantity, leaving only the intrinsic RMS. We have already made a single spectrum for each object by taking the average of all its available spectra. We account for the dispersion introduced by evolution and observational error by calculating the RMS variance of the available spectra for each object about the mean of that object. This quantity —the intra-object variation—when averaged over all the objects, gives an estimate of the dispersion that is *not* due to intrinsic differences between the supernovae. This dispersion is the dashed line in the middle panel

achieved by minimising a best-fit function for fixed magnitudes  $B$  and  $V_c$ ,

$$\epsilon(k) = (B - B_c)^2 + (V - V_c)^2 \quad (1)$$

$$= (a \log k + b - B_c)^2 + (c \log k + d - V_c)^2. \quad (2)$$

Differentiating with respect to  $\log k$  and setting the result equal to zero yields

$$k = \exp \left\{ \frac{a(B_c - b) + c(V_c - d)}{a^2 + c^2} \right\}. \quad (3)$$

The values of the coefficients are found as in the single-band case. Equation 3 allows us to determine *a priori* the scaling factor required to fix a spectrum near a chosen magnitude in both  $B$  and  $V$ .

of Figures 1 and 2. This dispersion is small compared to the dispersion between objects. Since the contribution from observational error is expected to only *increase* the scatter in the results we subtract (in quadrature) the observational scatter component from the overall RMS deviation. The remaining RMS, ideally all due to intrinsic diversity, is shown in the upper panel of Figures 1 and 2.

This method allows us to separate spectral diversity from scatter in absolute magnitudes. It will be sensitive to diversity in spectral features as well as colour variations — large scale spectral shape differences. The band to which we scale the spectrum will have the least diversity because we are effectively anchoring the dispersion to be lowest at this point. So when we are scaling to a fixed  $M_B$  the scatter is smallest between 4000Å and 5000Å, whereas when scaling to  $M_V$  the scatter is smallest between 5000Å and 6000Å. The change in the overall shape of the dispersion spectrum is slight, and the significant spectral features remain unaltered. In Figure 3 we compare the final results for scaling to the V band (upper panel) and B band (lower panel).

In Figure 4 we show a typical SN Ia spectrum at maximum light (Nugent, Kim & Perlmutter 2002). The spectrum peaks at 4000Å. Our analysis shows that blueward of this peak the UV edge of the spectrum shows more variety than the rest of the spectrum. Much of this is likely to be intrinsic SN Ia diversity, but it is also the region most susceptible to extinction and to observational flux errors. Rejecting the blue end of SN Ia spectra will reduce the scatter in SN Ia magnitudes that occurs both due to intrinsic SN variability and imperfect extinction correction. The Rayleigh-Jeans tail to the right of this peak, is a very stable region of the spectrum until the Si II feature around 6150Å produces a peak in variability. Beyond the Si II feature the diversity also appears to increase. However, this may be another indication of imperfect extinction correction.

We expect the dominant source of observational error that can not be accounted for by measuring intra-object dispersion to be due to extinction correction. By sampling the averaged object spectra with replacement many times we estimate the error in the extinction correction without making any assumptions about the error in colour excess values. Because we anchor the spectra to the B or V magnitudes of the supernovae (even when we are anchoring to the B or V magnitude of each supernova individually), any faulty extinction correction would show up as a bowl-shaped curve on our RMS vs wavelength plots (affecting high and low wavelengths equally - even though extinction preferentially affects short wavelengths). The curves in Figure 3 may be the most illustrative for this point, since we have scaled the spectra to a fixed magnitude in B and V (upper and lower), effectively minimising the scatter in these regions. An error in extinction correction shows up as a gradual increase in the scatter away from these regions.

In this analysis we are particularly concerned with (and sensitive to) small scale variation such as the variability of a particular spectral feature. Prominent spectral features correspond to regions of high scatter, most noticeably around the Si II line at 6150Å. Ideally we would avoid these regions when calculating the magnitudes of SNe Ia for use as standard candles. However, a large variation in a spectral line does not necessarily translate into a large variation in broad-band magnitude if the regions around the line are bright and stable, in which case the variability of these lines will find the greatest

utility as a tracer of different subsets of the SN Ia population.

In any real experiment we have a limited filter set, so cannot choose to observe the ideal region of every SN spectrum for the continuum of redshifts we need to cover. However, we can weight the error bars of our observations to favour those objects whose redshifts fortuitously allow one of our filters to cover the most stable region, and we can design filters narrow enough, and with sufficient overlap, to maximise the chance that a filter will cover only the most stable region (Davis et al. 2006).

Our analysis does not take into account any spectral differences between supernovae with different  $\Delta m_{15}$  values. When enough data is available it will be straightforward to apply this analysis to identify spectral features associated with wide or narrow light curves.

#### 4. MEASURING PECULIARITY

When using SNe Ia for cosmology we need to select the observed supernovae with the most homogeneous characteristics for use as standardisable candles. Most well observed supernovae exhibit some peculiar features, and their full utility in cosmology requires the characterisation of these differences. A significant step toward this is the creation of an objective measure of peculiarity that can act as an objective criterion for including an object in a sample population, and also identify subsets of SNe Ia with very similar properties. Here we outline two different methods for quantifying peculiarity and demonstrate them on the small data set currently available to us. These methods will benefit greatly from a much larger low- $z$  spectroscopic sample, such as is now being collected by a number of groups, including the Nearby Supernova Factory, the Canada France Hawaii Telescope Legacy Survey (CFHTLS), the European Supernova Collaboration and the Carnegie Supernova Project (Hamuy et al. 2005). In addition, applying these methods to the high- $z$  samples being collected by the ESSENCE collaboration, the CFHTLS and the SN Cosmology project will allow for tests of evolution in the demographics of the SN Ia population.

The first method uses a  $z$ -test to determine the degree to which a SN Ia deviates from the norm, and is particularly good at finding spectra with variations in regions which are usually stable, or spectra with strange continuum profiles. This means it is also good at picking out dubious extinction corrections. The second method uses principle component analysis and is particularly good at finding subsets of the population with similar characteristics. For example, it can pick out SNe Ia with high or low ejecta velocities by emphasising correlated differences between spectral features.

##### 4.1. Peculiarity Parameter

We use our calculation of intrinsic diversity to give a measure of the range within which supernovae can be considered normal at each wavelength. If an object deviates significantly from the average in a region of the spectrum which is very stable, such as the range from 4000Å to 6000Å, we might consider it ‘peculiar’. This can be quantified by assigning a  $z$ -score in each wavelength bin and then averaging the  $z$ -scores over some region, e.g. the entire spectrum or a band such as B or V. The  $z$ -score at wavelength  $\lambda$  is,

$$z_\lambda = \frac{f - \bar{f}}{\sigma}, \quad (6)$$

where  $f$ ,  $\bar{f}$  and  $\sigma$  are the flux of the object, the flux of the average spectrum and the dispersion of the average spectrum,

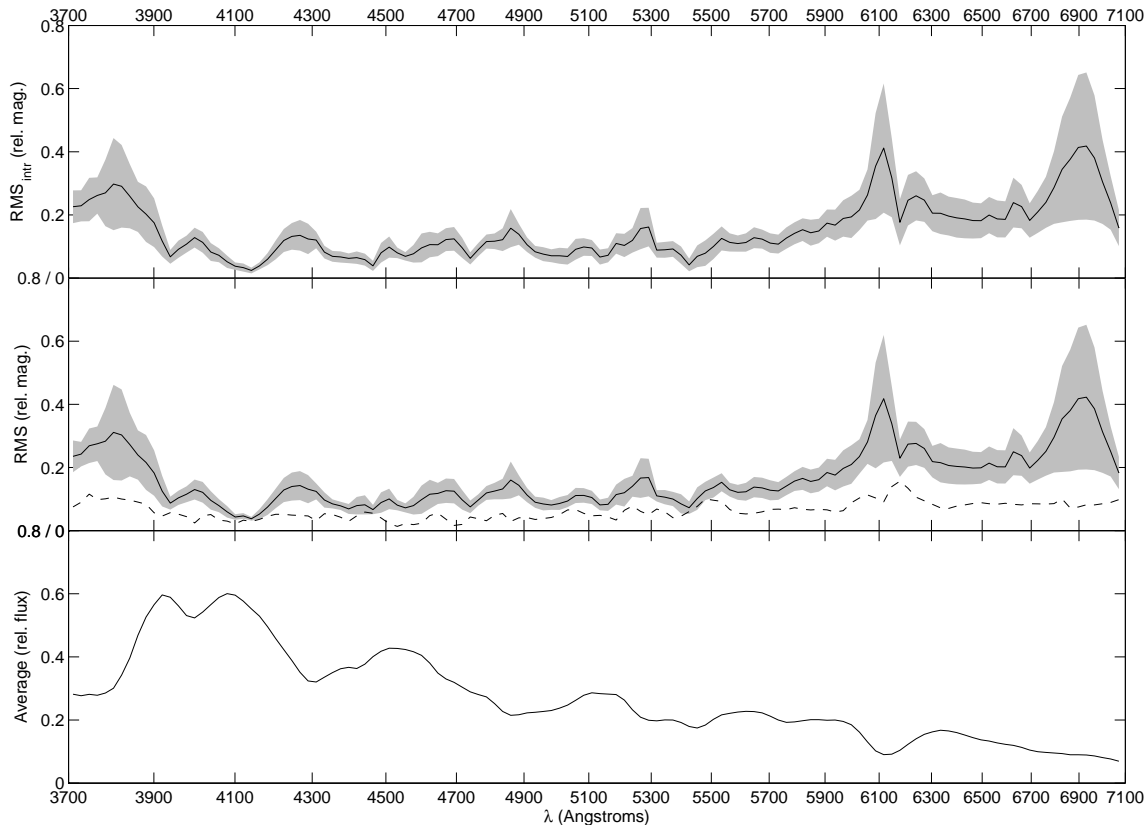


FIG. 1.— To calculate the diversity in SN Ia spectra as a function of wavelength we first calculate the average spectrum (bottom panel) and the RMS deviation from this average (middle panel, solid line). The uncertainty in this RMS is approximated by bootstrap resampling and is shown by the grey shading. The dashed line in the middle panel is the intra-object dispersion, and represents our estimate of the contribution from observational uncertainty. The upper panel shows our final result, which is the RMS minus this estimated observational dispersion. In this plot the spectra have been scaled to a fixed magnitude in the B band. This artificially lowers the scatter in the B-band region, centred around 4200Å. Large-scale shape variations in the spectra, would show up as a slow increase in the scatter away from this region (as we see here). Errors in extinction correction would also have this effect.

all at the wavelength  $\lambda$ . We define the ‘peculiarity parameter’,  $P$ , to be the absolute average of these terms over the  $n$  bins in the desired wavelength range,

$$P = \frac{1}{n} \sum_{\lambda} |z_{\lambda}|.$$

Subsets of this range, weighted by filter value, can be used to define the broadband peculiarity parameters, e.g. for  $B$ ,

$$P_B = \frac{1}{\sum_{\lambda} \tau_{\lambda}} \sum_{\lambda} \tau_{\lambda} |z_{\lambda}|,$$

where  $\tau_{\lambda}$  is the throughput of the  $B$  band filter at wavelength  $\lambda$ .

Figure 5 shows a histogram of  $P$  for the objects in our sample calculated according to this method using the wavelength range 3700 to 7100Å, based on the object averages for which the spectra were anchored in the B band. For this test, the average and RMS spectra are recalculated including observations from SN 1991bg and SN 1991T, previously classified as ‘peculiar’. The average spectrum changes negligibly when these objects are added. The peculiarity of 1991bg is made obvious by the test, from which we conclude that

the spectrum of this object departs markedly from the mean in a non-uniform (across  $\lambda$ ) manner. However SN 1991T, which is known to be bolometrically overluminous, shows little spectral peculiarity when scaled in magnitude to match other events.

To test the fidelity of this parameter, the histogram is compiled again using instead the spectra anchored in the V band. Figure 6 shows the recompiled histogram. Some slight rearranging occurs — notably the objects seem less bunched — however the prominence of 1991bg, and the relative lack of prominence of 1991T, are unchanged. We conclude that this parameter can distinguish events that exhibit peculiar broadband and spectral features, such as 1991bg-like events but does not distinguish objects like 1991T that are peculiar at wavelengths that also show significant diversity in normal supernovae.

#### 4.2. Principle Component Analysis

Principle component analysis (PCA) is a technique for identifying common characteristics in data with many variables (e.g. Francis and Wills 1999). PCA has been successfully applied to astronomical spectra in the past to identify different types of active galactic nuclei (Francis et al. 1992).

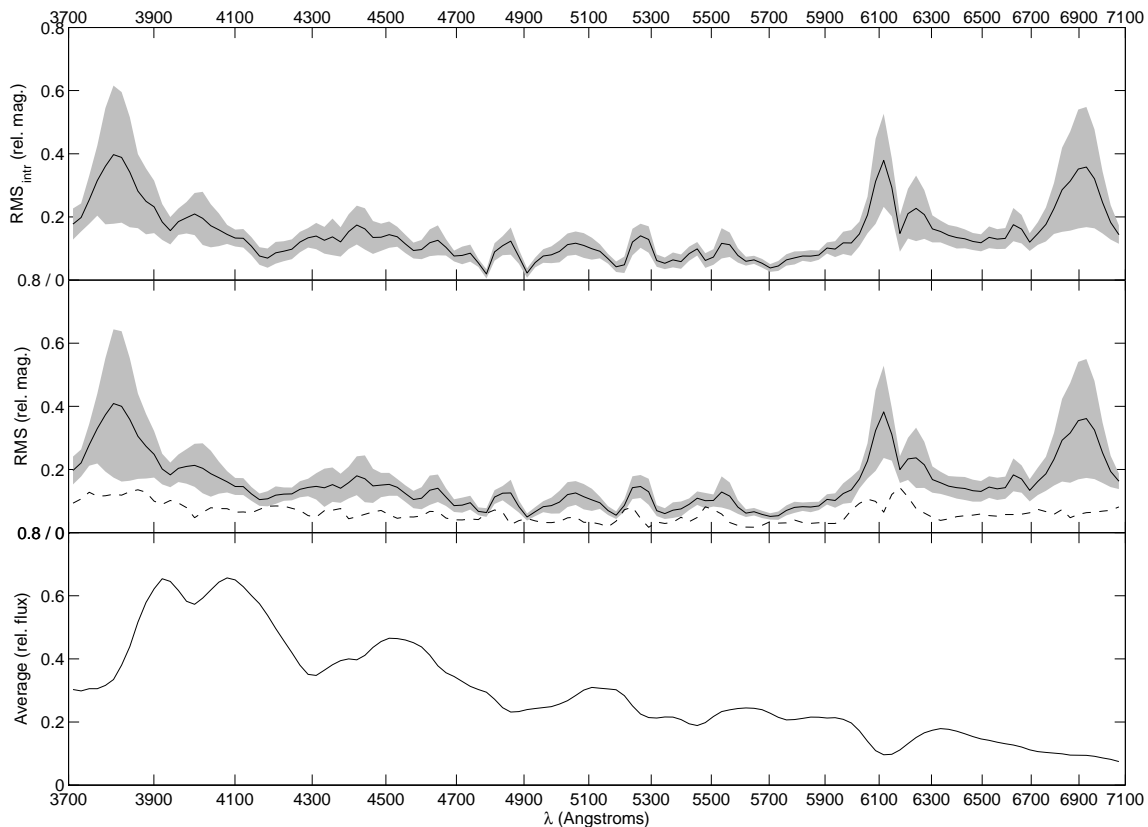


FIG. 2.— As for Figure 1, though here the spectra are scaled to have the same magnitude in the V band (centred around 5200Å), rather than the B band, as can be seen from the wavelength range of the region of lowest diversity. The same small-scale spectral features remain prominent, demonstrating the independence of the variance of these regions on the choice of anchor filter. For example, the variable strength (and position) of the Si II line observed at around 6150Å.

Here we demonstrate the concept on type Ia supernova spectra. This technique may be used in the future, with a larger sample set, as another method to identify subclasses of type Ia supernovae with similar properties. This is a major aim of several ongoing low-redshift supernova surveys and is important for the control of systematic errors in planned (and ongoing) high-redshift surveys that aim to measure the expansion history of our universe. We use the PCA technique developed by Francis et al. (1992) including their analysis code with some minor variations.<sup>5</sup>

We perform PCA on the sample of normal supernovae as outlined in Table 1, as well as the peculiar SNe 1991T and 1991bg. The result is shown in Fig. 7, where we have plotted the first and second principle components calculated for each supernova. This test successfully identifies these two supernovae as peculiar. Moreover, this method is able to distinguish 1991bg-like SNe from 1991T-like SNe because they each appear peculiar in a different principle component. This method therefore shows great promise for selecting subclasses of SNe Ia. Future work will perform this analysis on multi-epoch spectra, in which sub-class trends should be even more prominent.

<sup>5</sup> Many thanks to Paul Francis for supplying us with this code and running the first analysis.

One of the major uncertainties in supernova spectra arises due to extinction. Errors may be introduced by assuming the wrong amount of extinction, or because the applied extinction law is not a good representation of the effect of dust along the line of sight to the supernova. The size of dust particles along the line of sight will influence the shape of the extinction curve, and is a factor that is expected to change with environment. We propose a novel estimation of extinction error using PCA where the first component is given the form of the standard extinction law. Then applying PCA to non-extinction-corrected spectra should result in values of the first component that correlate with the extinction correction value calculated by traditional means. Applying PCA to extinction-corrected spectra may show residual power in the first component corresponding to incorrect extinction-correction. The results of this analysis will be presented in a forthcoming paper.

## 5. CONCLUSIONS

We have used published spectral data to calculate the diversity of type Ia supernova spectra close to maximum light as a function of wavelength between 3700Å and 7100Å. The region between 4100Å and 6000Å in the supernova’s rest frame is particularly stable. This is therefore the ideal region for calculating SN Ia magnitudes for use as standard candles.

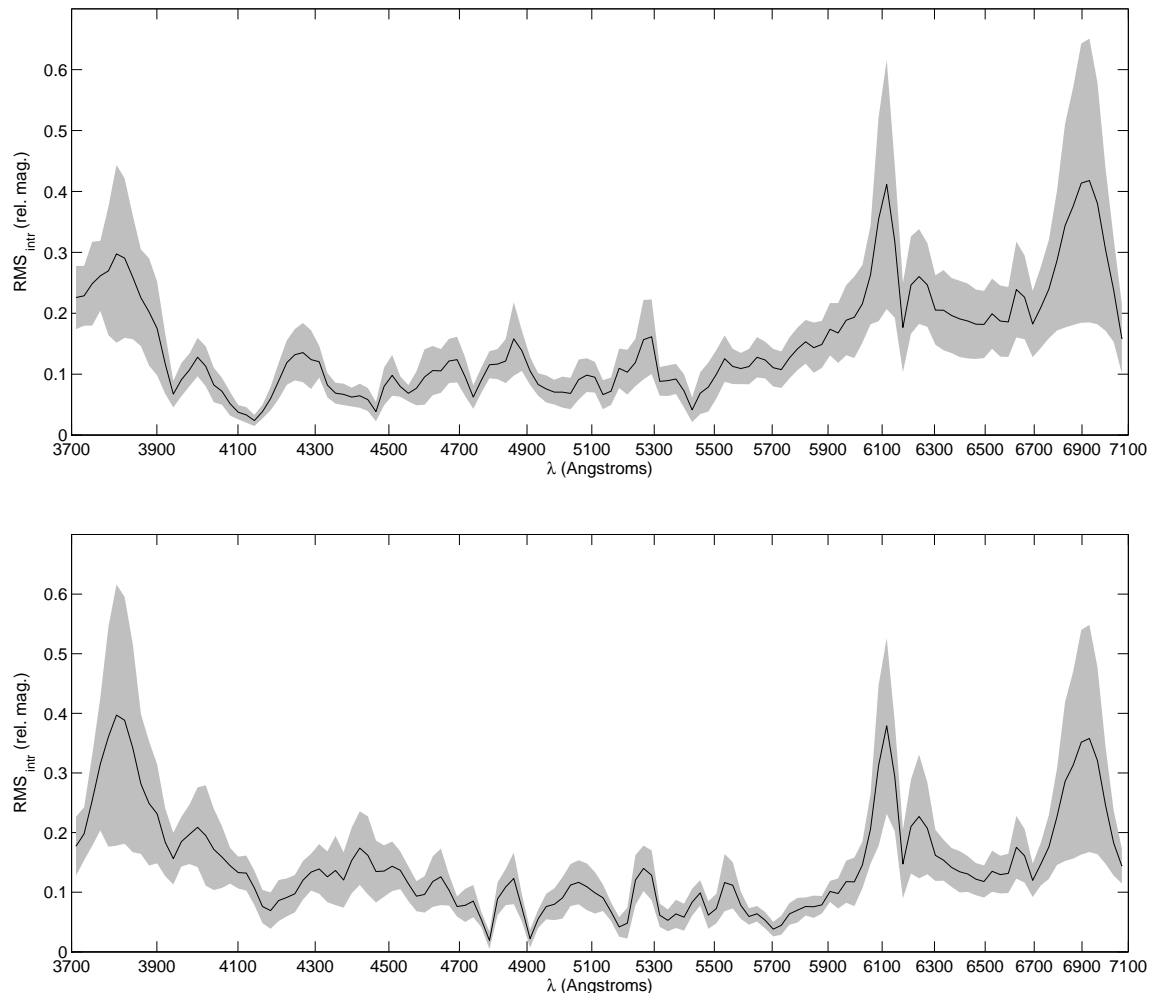


FIG. 3.— Intrinsic RMS (total RMS minus observational dispersion) for spectra normalised to the average absolute magnitude in B (upper) and V (lower).

There is an increase in supernova diversity below  $4100\text{\AA}$ . As we move blueward, extinction correction also becomes more uncertain and therefore the region below rest frame  $4100\text{\AA}$  should be avoided when using SN Ia as standardizable candles. Observations of this region remain useful for constraining theoretical models of SN Ia explosions, for example Nugent et al. (1995) showed the U band is a powerful tool for discriminating between different processes occurring in SNe Ia. Redward of the stable region the Si II line, typically observed at  $6150\text{\AA}$ , shows a large diversity. This feature has previously been used as a tracer of light-curve width (Nugent et al. 1995) and to identify peculiar SNe Ia (Branch et al. 1993a,b). Our analysis confirms that it is a variable feature of ordinary SNe Ia. Future work will extend this study to spectra over a wider epoch range.

We also demonstrated two methods for determining the peculiarity of type Ia supernovae, firstly by comparing their spectra to the average SN Ia spectrum while taking into account the typical variability of different spectral regions, and secondly using principle component analysis. Both methods

show promise for use as objective tests of peculiarity. PCA in particular may be a good way to objectively define sub-types of the SN Ia class.

The methods demonstrated here will benefit greatly from more spectroscopic data, not only more objects, but also extended wavelength coverage into the UV and IR. Although hundreds of supernovae have now been observed very well photometrically, the sample that have spectra published near maximum remains small. New data soon to be available from a variety of searches will enable a more robust analysis based on the methods demonstrated here.

#### ACKNOWLEDGMENTS

Many thanks are due to Paul Francis for sharing with us his principle component analysis code. We also thank the many observers who are responsible for obtaining this data. JBJ was supported by an Australian National University Summer Research Scholarship. TMD acknowledges the support of Lawrence Berkeley Laboratory.

#### REFERENCES

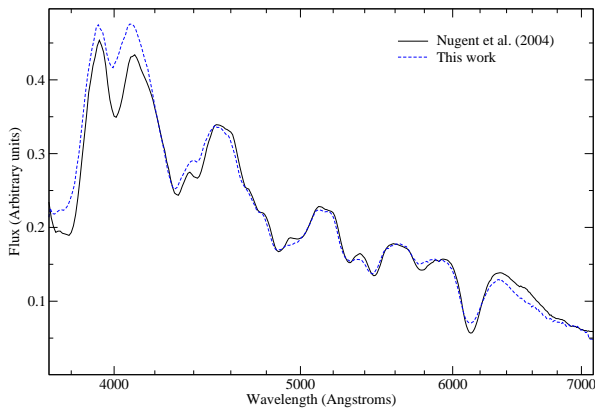


FIG. 4.— The industry standard for typical SN Ia spectra are the templates provided in Nugent, Kim & Perlmutter (2002). These are updated periodically, and the update of April 2005 can be found on [supernova.lbl.gov/~nugent/nugent\\_templates.html](http://supernova.lbl.gov/~nugent/nugent_templates.html). Here we overplot our average spectrum on the Nugent template for a SN Ia at maximum light. The agreement is good. Our analysis shows that the UV edge of the spectrum, below the peak around  $4100\text{\AA}$ , shows an increased diversity among SNe Ia. (Whether this continues below the limit of our useful data, at  $3700\text{\AA}$ , is an open question.) This also approximately corresponds to where our average spectrum starts to deviate significantly from the Nugent template - corresponding to the greater uncertainty about the typical spectrum of this region. We have shown that the Rayleigh-Jeans tail to the right of the peak is a very stable region of the spectrum, until we reach the Si II feature at  $6150\text{\AA}$ . This is therefore the best region of the spectrum to use as a standard candle for cosmological parameter estimation.

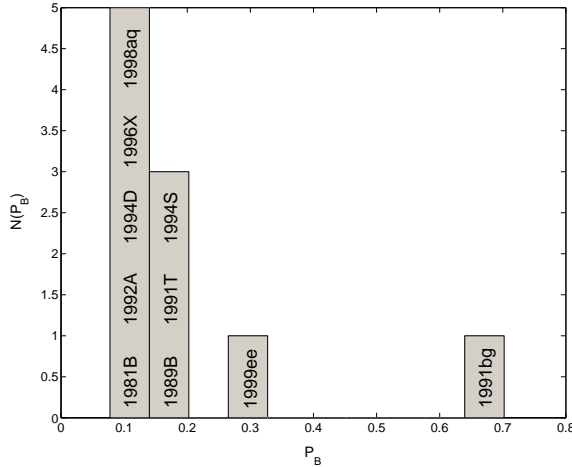


FIG. 5.— Histogram of peculiarity parameter,  $P$ . Spectra have been scaled to the average absolute magnitude in the B band. The average spectrum from which deviation is measured is composed of average spectra from the objects listed excluding 1991bg and 1991T.

Branch, D. et al. 1983, *ApJ*, 270, 123 (Br83)  
 Branch, D., van der Bergh, S. 1993, *AJ*, 105, 2231  
 Branch, D., Fisher, A., & Nugent, P. 1993, *AJ*, 106, 2383  
 Branch, D. et al. 2003, *AJ*, 126, 1489 (Br03)  
 Davis, T. M., Schmidt, B. P., & Kim, A. 2006, *PASP*, in press  
 Efron, B., 1982, *The Jackknife, the Bootstrap and other resampling plans*, CBMS-NSF Regional Conference Series in Applied Mathematics, Philadelphia: Society for Industrial and Applied Mathematics (SIAM)  
 Francis, P. J., Hewett, P. C., Foltz, C. B. & Chaffee, F. H. 1992, *ApJ*, 398, 476  
 Francis, P. J. & Wills, B. J. 1999, *Quasars and Cosmology*, ASP Conference Series 162, Eds Ferland, G. & Baldwin, J., p. 363  
 Hamuy, M., Phillips, M. M., Schommer, R. A., Suntzeff, N. B., Maza, J., & Aviles, R. 1996, *AJ*, 112, 2391  
 Hamuy, M. et al. 2002, *AJ*, 124, 417

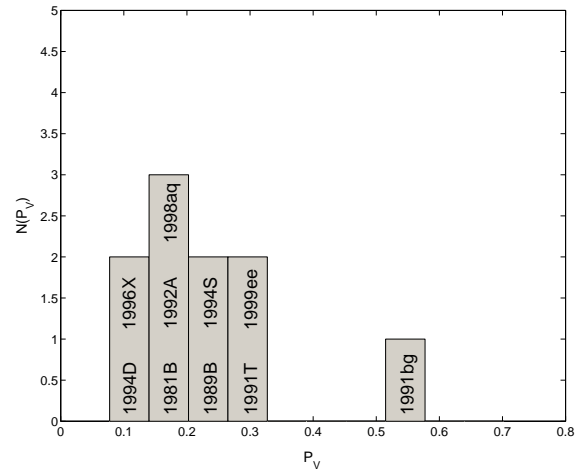


FIG. 6.— Histogram of peculiarity parameter,  $P$ , with the average spectrum additionally excluding 1999ee. Spectra have been scaled to the average absolute magnitude in the B band.

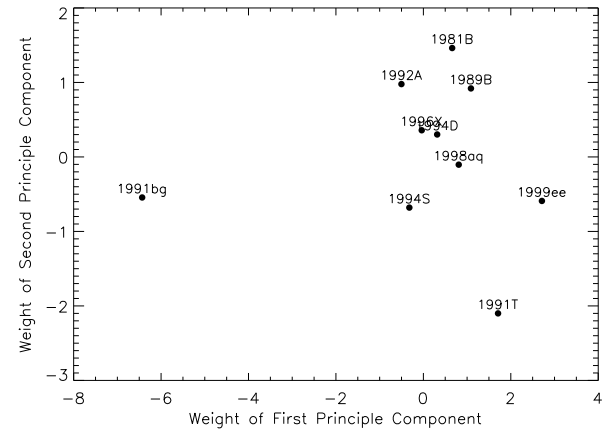


FIG. 7.— For each SN spectrum we plot the weights of the first and second components of a principle component analysis. The underluminous event, SN1991bg, is identified as peculiar in the first principle component, and the overluminous SN 1991T is the most peculiar SN in the second principle component. This is particularly interesting because the spectra have been scaled to the same overall flux between  $3700\text{\AA}$  and  $7100\text{\AA}$ , so the peculiarity that is apparent here is a difference in the shape and features of the spectrum, rather than simply a shift in the luminosity.

Hamuy, M. et al. 2005, *PASP*, in press  
 Kirshner, R. P., et al. 1993, *ApJ*, 415, 589 (Ki93)  
 Knop, R. A. et al. 2003, *ApJ*, 598, 102 (Kn03)  
 Leibundgut, B., Kirshner, R. P., Filippenko, A. V., Shields, J. C., Foltz, C. B., Phillips, M. M., & Sonneborn, G. 1991, *ApJL*, 371, L23 (L91)  
 Leibundgut, B. et al. 1993, *AJ*, 105, 301 (Le93)  
 Nugent, P., Phillips, M., Baron, E., Branch, D. and Hauschildt, P. 1995, *ApJL*, 455, L147  
 Nugent, P., Kim, A., & Perlmutter, S. 2002, *PASP*, 114, 803  
 Patat, F., Benetti, S., Cappellaro, E., Danziger, I. J., della Valle, M., Mazzali, P. A., & Turatto, M. 1996, *MNRAS*, 278, 111 (Pa96)  
 Phillips, M. M. 1993, *ApJL*, 413, L105  
 Phillips, M. M., Lira, P., Suntzeff, N. B., Schommer, R. A., Hamuy, M., & Maza, J. 1999, *AJ*, 118, 1766 (Ph99)  
 Saha, A., Sandage, A., Tammann, G. A., Dolphin, A. E., Christensen, J., Panagia, N., & Macchetto, F. D. 2001, *ApJ*, 562, 314 (Sah01)  
 Salvo, M. E., Cappellaro, E., Mazzali, P. A., Benetti, S., Danziger, I. J., Patat, F., & Turatto, M. 2001, *MNRAS*, 321, 254 (Sal01)  
 Savage, B. D., & Mathis, J. S. 1979, *ARA&A*, 17, 73  
 Stritzinger, M. et al. 2002, *AJ*, 124, 2100 (St02)

James, Davis, Schmidt & Kim  
Tripp, R. 1998, A&A, 331, 815  
Vaughan, T. E., Branch, D., Miller, D. L., & Perlmutter, S. 1995, ApJ, 439,  
558  
Wang, L., Goldhaber, G., Aldering, G., & Perlmutter, S. 2003, ApJ, 590, 944

Wang, X., Wang, L., Zhou, X., Lou, Y.-Q., & Li, Z. 2005, ApJ, 620, L87  
Wells, L. A. et al. 1994, AJ, 108, 2233 (We94)